Carbohydrate Polymers 90 (2012) 1046–1054

Contents lists available at SciVerse ScienceDirect

Carbohydrate Polymers

journal homepage: www.elsevier.com/locate/carbpol

Multi-morphological self-assembled structures in water of a biodegradable β-cyclodextrin-based copolymer

Ming-Wei Jiang, Cheng-Gong Guo, Liang Wang, Cai-Qi Wang*

College of Chemistry and Chemical Engineering, Graduate University of Chinese Academy of Sciences, Beijing 100049, PR China

ARTICLE INFO

Article history:
Received 2 December 2011
Received in revised form 28 May 2012
Accepted 14 June 2012
Available online 23 June 2012

Keywords:
Biodegradable
Caprolactone
Self-assembly
β-Cyclodextrin
Rigid-coil

ABSTRACT

A rigid-coil β-cyclodextrin-poly (ε-caprolactone) (CD-PCL) copolymer was synthesized in which biodegradable flexible multi PCL arms were selectively connected onto the wide side of the rigid torus-shaped β-CD through ring-opening polymerization (ROP) of ε-caprolactone (CL) and protection/deprotection technique of β-cyclodextrin (β-CD) *via* trimethylsilyl groups. ^{1}H NMR, FT-IR, and GPC analysis confirmed the "jellyfish-like" branched architecture of CD-PCL copolymers. The self-assembled structures in water of the amphiphilic CD-PCL copolymer were investigated by transmission electron microscopy (TEM), dynamic light scattering (DLC) and viscometry. The results showed that CD-PCL could self-assemble into multi-morphological aggregates such as spheres, rods, vesicles, vesicular clusters and vesicular network in water. Interestingly, hierarchical stripe structure was observed in the formed vesicular network, which was driven by the crystallization of PCL segment in micelles. Moreover, the inclusion ability of copolymer micelles with ferrocenecarboxylic acid was investigated by UV.

1. Introduction

Copolymers are widely explored for their ability to self-assemble into micellar aggregates with different morphologies in selective solvents (Agut, Brûlet, Schatz, Taton, & Lecommandoux, 2010; He et al., 2009; Hickey, Haynes, Kikkawa, & Park, 2011; Jain & Bates, 2003; Neiser et al., 2004) as well as their applications in the field of biotechnology and pharmaceutics (Discher & Eisenberg, 2002; Ren, Feng, Zhang, Li, & Li, 2011; Rösler, Vandermeulen, & Klok, 2001; Song et al., 2010). Besides the molecular composition of the copolymers, the molecular topological architectures including linearity, branching, rigidity and flexibility are very important factors in determining the self-assembled micellar morphology. Indeed, the self-assembly of rigid-coil copolymers is directed not only by the microphase separation of the blocks but also by the tendency of the rigid segments to form anisotropic liquid-crystalline or crystalline domains. This competition process can lead to morphologies that are distinctly different from those that are commonly observed for conventional coil–coil copolymers (Chen, Thomas, Ober, & Mao, 1996; Jenekhe & Chen, 1999; Liu, Lin, Kuo, Lin, & Chen, 2011; Park, Moon, Seo, Choi, & Kim, 2010). Thus, rigid-coil copolymers represent an attractive class of building blocks for the preparation of self-assembled nanostructures (Ho, Lee, Dai, Segalman, & Su, 2009; Junnila et al., 2010; Klok & Lecommandoux, 2001; Lee, Cho, & Zin, 2001).

Branched copolymers as well as linear block copolymers can self-organize into micelles in selective solvents. When compared with linear block copolymers, branched copolymers can add additional functionalities to that provided by the polymer backbone, which can be accessed following the self-assembly process (Breitenkamp & Emrick, 2003; Sato et al., 2005). However, in most cases, branched copolymers tend to form compound spherical micelles (Akiyoshi, Deguchi, Tajima, Nishikawa, & Sunamoto, 1997; Jeong, Kang, Yang, & Kim, 2003; Kuroda, Fujimoto, Sunamoto, & Akiyoshi, 2002; Philippova et al., 2001) or unimolecular micelles (Kikuchi & Nose, 1996; Yusa, Sakakibara, Yamamoto, & Morishima, 2002) whereas linear block copolymers can organize into abundant morphologies such as spheres, rods, vesicles, *etc.* (Cheng, Huang, Tang, Chen, & Xi, 2005; Jenekhe & Chen, 1998; Zhang & Eisenberg, 1996). It seems difficult for a branched copolymer to form different morphologies in a selective solvent and this creates the impression that the branched structure of a branched copolymer precludes morphological diversity. Actually, nearly all the earlier studies on the synthesis and self-assembly of branched copolymers focus on coil–coil branched copolymers with random branch lengths and density. It is possible that the randomly branched structure of a coil–coil branched copolymer precludes morphological diversity. If the molecular structure of a branched copolymer could be properly manipulated or rigid segments introduced into a branched copolymer, it should be possible for a branched copolymer to assemble into a wide range of morphologies in selective solvents (Borisov & Zhulina, 2005; Duan, Kuang, Wang, Chen, &

* Corresponding author at: College of Chemistry and Chemical Engineering, Graduate University of the Chinese Academy of Sciences, 19A Yuquan Road, Beijing 100049, PR China. Tel.: +86 10 88256677; fax: +86 10 88256092.
E-mail address: wang-caiqi@gucas.ac.cn (C.-Q. Wang).

0144-8617/$ – see front matter © 2012 Elsevier Ltd. All rights reserved.
http://dx.doi.org/10.1016/j.carbpol.2012.06.041

Jiang, 2003; Kim, Huh, & Jo, 2003). In contrast to those extensive investigations on the micellization of flexible and linear block copolymers, relatively few studies have been conducted on the self-assembled nanostructures of branched copolymers with well-defined and rigid-coil molecular architectures (Cai, Lin, Chen, & Tian, 2009; Wang, Li, & Guo, 2005). Thus, we are particularly interested in branched copolymers consisting of controlled branched structures and rigid-coil chains. It is expected that the integration of the above two factors may lead to non-spherical self-assembled morphologies.

Over the past few years, biodegradable and biocompatible saccharide-based branched copolymers have attracted much attention because of their potential application as biomimetic materials (Hu et al., 2002; Nouvel et al., 2004; Ouchi, Kontani, & Ohya, 2003). β-Cyclodextrin (β-CD) is a cyclic oligosaccharide with seven D-glucose units linked by α-1,4-glucose bonds. This oligosaccharide has a unique rigid architecture of truncated cone in which the primary hydroxyl groups are directed to the narrow side and the secondary hydroxyl groups are on the wide side of the torus. Due to the arrangement of the functional groups, the torus-shaped β-CD forms hydrophilic outer surface and hydrophobic cavity in which suited guest molecules can be encapsulated. So β-CD is not only a suitable backbone to design well-defined branched copolymers but also a suitable rigid building block to drive the formation of highly ordered structures. However, well-defined saccharide-based branched copolymers are generally difficult to synthesize due to the existence of primary and secondary hydroxyl groups. Recently, the protection and deprotection of partial hydroxyl groups *via* trimethylsilyl (TMS) and tert-butyldimetylsilyl (TBDMS) groups have been successfully adopted in the preparation of saccharide-based branched copolymers with controlled structures in a homogeneous system (Gou, Zhu, & Shen, 2010; Qiu, Wang, Shen, & Jiang, 2011; Wang, Dong, & Tan, 2003; Wang et al., 2005; Ydens et al., 2000).

Thus, in this paper, a facile strategy to prepare rigid-coil biodegradable β-CD based branched copolymers with controlled structures was successfully developed through the combination of ring-opening polymerization (ROP) and protection/deprotection technique of β-CD *via* trimethylsilyl groups. Herein, biodegradable poly (ε-caprolactone) (PCL) as flexible hydrophobic branch was selectively connected onto the wide side of the rigid hydrophilic torus-shaped β-cyclodextrin. Various self-assembled morphologies were observed due to the unique rigid-coil branched structure. Such nanostructures are expected to be applicable as potential drug carrier materials.

2. Experimental

2.1. Materials and methods

2.1.1. Materials

β-Cyclodextrin (Beijing Solarbio Science & Technology Co., Ltd., PR China) was recrystallized twice from water and vacuum-dried at 60 °C under vacuum before use. ε-Caprolactone (CL, Acros Organics, 99%) was dried over CaH_2 for 48 h, distilled under reduced pressure with the fraction collected at 96–98 °C (5 mmHg), and stored under an inert atmosphere. Stannous octoate ($Sn(Oct)_2$) (Alfa-Aesar) was used without any further purification. p-Xylene and DMSO were dried by refluxing over CaH_2 and Na/benzophenone complex and distilled just before use. Boron trifluoride diethyl etherate ($BF_3{\cdot}Et_2O$, 48% BF_3), 1,1,1,3,3,3-hexamethyldisilazane (HMDS), ferrocenecarboxylic acid (FcAc) and other regents were purchased from commercial sources and used as received.

2.1.2. Methods

^{1}H NMR analysis was carried out on a JOEL JNM-ECA600 spectrometer in $CDCl_3$, in DMSO-d_6, or in D_2O at room temperature (solvents without TMS). FT-IR measurements were carried out on AVATAR 360 FT-IR spectrometer (Thermo Nicolet). The samples for FT-IR measurement were prepared by dispersing the powdered in KBr and compressing the mixtures to form disks. Molecular weight (M_n) and molecular weight distribution (M_w/M_n) were measured with a Viscotek TDA GPC instrument equipped with tetrahydrofuran (THF) as the mobile phase and polystyrene as calibration standard. Fluorescence was measured with a Fluorolog-3, horiba Jobin Yvon spectrofluorometer. The UV–vis spectra and kinetics were recorded on a UV-2550 spectrophotometer (Shimadzu, Japan), using 1-cm path length quartz cuvetts for measurements.

Transmission electron microscopy (TEM) was performed on a TECNAI T20 electron microscope. Samples for TEM measurement were prepared by ultrasonic dispersion of the micelle solution onto 200-mesh gilder copper TEM grids and air-dried at room temperature. All grids were negatively stained by 2 wt% phosphotungstic acid. The size distribution of the aggregates was analyzed by a Malvern 3000HS Zetasizer using a monochromatic coherent He–Ne laser (633 nm) as the light source and a detector that detected the scattered light at an angle of 90°. The viscosity measurements were made in an Ubbelohde viscometer, which was placed in a thermostatically controlled bath with a precision of 25 ± 0.1 °C. The measurements were repeated at least three times and the times obtained were arithmetically averaged, and then converted to the reduced viscosity (η_{sp}/c) according to the equation of $\eta_{sp}/c = (t - t_0)/t_0C$, where t and t_0 are the flowing time of copolymer water solution and solvent water, respectively. The concentration of the copolymer solution in water is in the range of 0.0005–0.2 mg/ml.

2.2. Synthesis of CD-PCL copolymers

2.2.1. Trimethylsilylation of β-cyclodextrin

Trimethylsilylated cyclodextrin (TMSCD) was synthesized from CD and HMDS and characterized, as described in our recent publication (Qiu et al., 2011). The TMS substitution degree (DS_{TMS}) of TMSCD in the present study was DS = 71.9%.

The trimethylsilyl substitution degree (DS_{TMS}) of β-cyclodextrin was determined using the following equation:

$$DS_{TMS}\,(\%) = \frac{7I_{Si(Me)_3}}{9I_{H_{(1,2,3,4,5,6a,6b)}}} \times 100 \quad (1)$$

where $I_{Si(Me)_3}$ and $I_{H_{(1,2,3,4,5,6a,6b)}}$ are the integral areas of the methyl proton signals of the TMS groups and those of the methine proton (H-1,2,3,4,5) and methylene proton (H-6a,6b) signals of the glucose unit, respectively.

IR (KBr, powder, cm^{-1}): 3440 (O—H), 2960 (C—H), 2901 (C—H), 1250 (Si—CH_3), 1160–1000 (pyranose), 881, 845 (Si—CH_3). ^{1}H NMR ($CDCl_3$, 600 MHz): 0.1–0.4 (9H, CH_3—Si), 3.25 (1H, H-6a), 3.46 (1H, H-5), 3.53 (2H, H-2, H-3), 3.69 (1H, H-6b), 3.78 (1H, H-4), 4.65 (1H, —O—H[3]), 4.77 (1H, H-1). GPC(THF): M_n = 1646, M_w/M_n = 1.04.

2.2.2. ROP of CL from trimethylsilylated β-cyclodextrin (TMSCD)

TMSCD-PCL copolymers were synthesized by ring-opening polymerization (ROP) of ε-caprolactone using $TMSCD_{DS=71.9\%}$ as the multifunctional initiator in the presence of $Sn(Oct)_2$. A typical polymerization procedure was as follows. $TMSCD_{DS=71.9\%}$ (1.0 g, 2.6 mmol of OH group) was dried at 70 °C under reduced pressure overnight and transferred into a dried two-necked round-bottom flask equipped with a stopcock and a rubber septum, purged with nitrogen. Then dry p-xylene (concentration ~20%) and varying amounts of ε-CL (3.56 g and 5.33 g respectively) and a magnetic

Table 1
Characterization of CD-PCL copolymers.

Sample	$[CL]_0/[OH]$ [a] (molar ratio)	Conv. (%)	$\overline{DP_{PCL,cal}}$ [b]	$\overline{DP_{PCL,NMR}}$ [c]	F_{PCL} [b](grav%)	$M_{n,Cal}$ [b]	$M_{n,GPC}$ [d] (g mol^{-1})	PDI[b]
TMSCD-PCL_{12}	12	98.6	12	26	78.6	10,438	9893	1.30
TMSCD-PCL_{18}	18	98.8	18	33	84.6	14,542	12,099	1.70
CD-PCL_{12}	–	–	12	21	87.8	9343	9218	1.70
CD-PCL_{18}	–	–	18	30	91.5	13,447	9342	1.32

CD-PCL with different PCL arm length were denoted CD-PCL_s, wherein the suffix of s means the polymerization degree of a single PCL arm attached to glucose unit and determined by the initial feed molar ratio of CL and every hydroxyl group of TMSCD. DS of the TMSCD employed was 71.9%.

[a] Calculated from the equation: $[OH] = 21 \times (1 - DS) \times [TMSCD]$.

[b] Calculated from the feeding molar ration of $[CL]_0/[OH]$[a].

[c] Calculated by the results of ^{1}H NMR.

[d] Estimated.

stirring bar were added to the flask under a nitrogen atmosphere. After $TMSCD_{DS=71.9\%}$ was completely dissolved in xylene, the flask was connected to a Schlenk-line, where an exhausting-refilling process was repeated three times. A total amount of 10 mg $Sn(Oct)_2$ in 1 ml dry xylene was added to the mixture, and the exhausting-refilling process was carried out again. The reactor was heated in an oil bath at 120 °C for 24 h solution polymerization. The crude polymer was dissolved in $CHCl_3$ and poured into excess methanol to precipitate the product, which was dried *in vacuo* to constant weight. Yield: 4.58 g (98%).

The average polymerization degree ($\overline{DP_{PCL}}$) of ε-caprolactone connected onto every hydroxyl group of the TMSCD backbone was determined by two methods. One is using the initial feed molar ratio of CL and every hydroxyl group of TMSCD. The other is by ^{1}H NMR using the following equation:

$$\overline{DP_{PCL}} = \frac{9I_{H_c}}{2I_{Si(Me)_3}} \times \frac{DS_{TMS}}{1 - DS_{TMS}} \quad (2)$$

where I_{H_c} is ^{1}H NMR integral intensity of CL repeating units calculated from the methylene protons at 2.3 ppm (—O—C(O)—CH_2—) and $I_{Si(Me)_3}$ is ^{1}H NMR integral intensity of trimethylsilyl units calculated from the methyl protons at 0.1 ppm (—$Si(CH_3)_3$). The corresponding results are shown in Table 1.

IR (KBr, powder, cm^{-1}): 3430 (O—H), 2950 (C—H), 2866 (C—H), 1730 (C=O), 1240 (Si—CH_3), 1180–1000 (pyranose), 880, 843 (C—Si). ^{1}H NMR (600 MHz, CDCl3, δ, ppm): 4.1 (2H, —CH_2—O—C(O)—), 3.0–4.9 (H-1, -2, -3, -4, -5, and -6 of pyranose), 2.3 (2H, —O—C(O)—CH_2—), 1.6 (4H, —O—C(O)—C—CH_2—, —CH2—C—O—C(O)—), 1.3 (2H, —C(O)—C—C—CH_2—C—C—O—), 0.1 (9H, —O—$Si(CH_3)_3$).

2.2.3. Deprotection of TMSCD-g-PCL

The protected hydroxyl groups on the β-CD backbone were recovered by desilylation of the trimethylsilyl ether groups in the presence of $BF_3{\cdot}Et_2O$. Typically, $BF_3{\cdot}Et_2O$ (0.5 ml, 2 mmol) in 10 ml of anhydrous CH_2Cl_2 was added dropwise to a solution of TMSCD-PCL (1.0 g, 0.95 mmol of TMS group) in 80 ml of anhydrous CH_2Cl_2 under stirring. The reaction mixture was stirred at room temperature for 12 h under a nitrogen atmosphere and then washed successively with $NaHCO_3$ (100 ml, 1 M) and distilled water. The organic phase was dried over anhydrous $MgSO_4$. The concentrated solution was poured into cold methanol to precipitate the product. The resulting white solid was dried *in vacuo* at room temperature for 24 h. Yield: 0.8 g (80%).

IR (KBr, powder, cm^{-1}): 3440 (O—H), 2950 (C—H), 2866 (C—H), 1730 (C=O), 1180–1000 (pyranose). ^{1}H NMR (600 MHz, $CDCl_3$, δ, ppm): 4.1 (2H, —CH_2—O—C(O)—), 3.0–4.9 (H-1, -2, -3, -4, -5, and -6 of pyranose), 2.3 (2H, —O—C(O)—CH_2—), 1.6 (4H, —O—C(O)—C—CH_2—, —CH2—C—O—C(O)—), 1.3 (2H, —C(O)—C—C—CH_2—C—C—O—).

2.2.4. Preparation of CD-PCL Micelles and CD-PCL/FcA

The obtained CD-PCL_{18} copolymer was initially dissolved in common solvent DMF to form a series of copolymer solutions with different initial concentrations (0.01–8.0 mg/ml) at room temperature. 5 ml Deionized water was added dropwise to 2 ml CD-PCL_{18} solutions. The solution was stirred for another 2 h unless otherwise noted, and then a twofold excess of water (5 ml) was added to quench the resulting micelles before dialysis against water to remove the remaining DMF solvent. After 48 h, the volume of the solution increased to about 12 ml. The final concentration of the obtained copolymer solution in water varied from 0.002 mg/ml to1.3 mg/ml. Similarly, a 10 ml solution of 2.0 mg/ml CD-PCL_{18} in DMF was slowly dropped into 10 ml of FcA aqueous media (2.0 mg/ml) under sonication, followed by dialysis against deionized water. After 48 h, the volume of the solution increased to 40 ml with the addition of deionized water to obtain an aggregate solution with a concentration of 1.0 mg/ml for further experiments.

The critical aggregate concentration (CMC) of CD-PCL_{18} in water was measured by the fluorescent probe method. 5 μl of 6×10^{-3} mg/ml pyrene solution in acetone was added to CD-PCL_{18} aqueous solutions with different concentrations and the solutions were sonicated for 10 min before fluorescence emission measurements.

3. Results and discussion

3.1. Synthesis and characterization of CD-PCL copolymers

The preparation of biodegradable CD-PCL copolymers with controlled branched structures was carried out according to the following three steps illustrated in Scheme 1. TMSCD was firstly synthesized from β-CD and hexamethyldisilazane (HMDS) in DMSO at 80 °C, in which the number of —OH groups substituted by trimethylsilyl groups (defined as DS_{TMS}) was controlled by the adjustment of the molar ratio of HMDS and CD. When the molar ratio of HMDS and CD reached 0.7, TMSCD with high DS (DS = 71.9%) was obtained, which indicated that about 15 hydroxyl groups on the β-CD backbone were substituted by TMS groups and there remained about 6 free secondary hydroxyl groups at the third position (3-OH) on the β-CD backbone, due to the relatively weak reactivity. These remaining secondary hydroxyl groups may provide the initiating sites for the next copolymerization.

The chemical structure of $TMSCD_{DS=71.9\%}$ was confirmed by ^{1}H NMR. As shown in Fig. 1a, it clearly shows that there are additional methyl proton signals (—O—$Si(CH_3)_3$, 0.1–0.4 ppm) of TMS groups besides the methine proton signals (H-1, 4.8 ppm) and the methylene protons signals (H-2, 3, 4, 5, 6a, 6b, 3.0–4.0 ppm) of the parent β-CD glucose unit. At the same time, only the signal of hydroxyl proton at the third position (3-OH, 4.5 ppm) can be observed while the signals derived from the hydroxyl protons at the second and sixth position (2, 6-OH, 5.7∼5.8 ppm) on the β-CD backbone disappear. This observation confirms that the 2-OH and 6-OH groups of

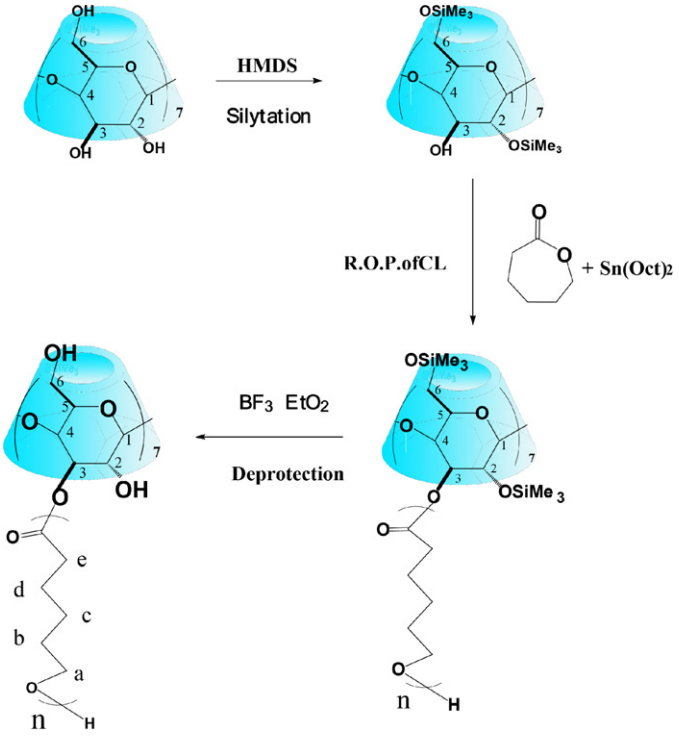

Scheme 1. Synthetic route of biodegradable cyclydextrin-poly(ε-caprolactone) copolymer.

β-CD glucose units were successfully substituted by TMS groups. According to the integral ratio of peak areas of the methyl protons of the TMS groups and those of the protons (H-1,2,3,4,5, 6a,6b) of the β-CD monosaccharide residue, the DS_{TMS} of TMSCD is calculated as about 71.9%, meaning that there remain six free secondary hydroxyl groups (3-OH) on the wide side of the torus-shaped β-CD.

β-CD only dissolves in polar solvents such as DMSO and water. But the obtained $TMSCD_{DS=71.9\%}$ achieved solubility in a variety of organic solvents, such as chloroform, acetone, THF and p-xylene. Therefore, the ring-opening polymerization of ε-caprolactone connected onto the wide side of the $TMSCD_{DS=71.9\%}$ was carried out in a homogeneous xylene solution with the remained 6 free secondary hydroxyl groups (3-OH) as initiating sites and $Sn(Oct)_2$ as catalyst. The reaction temperature was selected at 120 °C to reduce the transesterification and nearly all the CL were ring-opening polymerized (yields > 98%) when the reacting time reached 24 hour. Assuming that all the remaining free hydroxyl groups of the $TMSCD_{DS=71.9\%}$ can effectively initiates the ROP of CL, the average length of PCL branches can be calculated. And two TMSCD-PCL_s copolymers with different PCL branch lengths ($s = \overline{DP_{PCL}}$) were prepared by tuning the molar ratio of CL and hydroxyl group of $TMSCD_{DS=71.9\%}$ and characterized by ^{1}H NMR and GPC. The corresponding results are shown in Figs. 1 and 2 and Table 1.

Fig. 1c exhibits a representative TMSCD-PCL_{18} ^{1}H NMR spectrum. It clearly shows that besides the methlene proton signals of PCL chains (Hc-f, 3.9 ppm, 2.5 ppm, 1.5 ppm, 1.2 ppm), there are additional proton signals of the TMSCD moiety (H of pyranose and —O—Si(CH_3)$_3$, 3.0–5.0 ppm and 0.1 ppm). The average polymerization degree ($\overline{DP_{PCL}}$) of ε-caprolactone connected onto every hydroxyl group of the $TMSCD_{DS=71.9\%}$ backbone was determined by two methods. One is using the integral ratio of peak areas of the methylene protons (—O—C(O)—CH_2—, 2.35 ppm) of CL repeating units to those of the methyl protons of trimethylsilyl units (—Si(CH_3)$_3$, 0.1 ppm) in the TMSCD-PCL ^{1}H NMR spectrum. The other is using the initial feed molar ratio of CL and hydroxyl group of $TMSCD_{DS=71.9\%}$. It can be observed that $\overline{DP_{PCL}}$ determined by ^{1}H NMR even exceeds that calculated from the initial feed molar ratio, as is depicted in Table 1. The discrepancy is more evident for copolymers rich in PCL. The result is consistent with that of the poly (ε-caprolactone)-grafted dextran copolymers reported by Isabelle

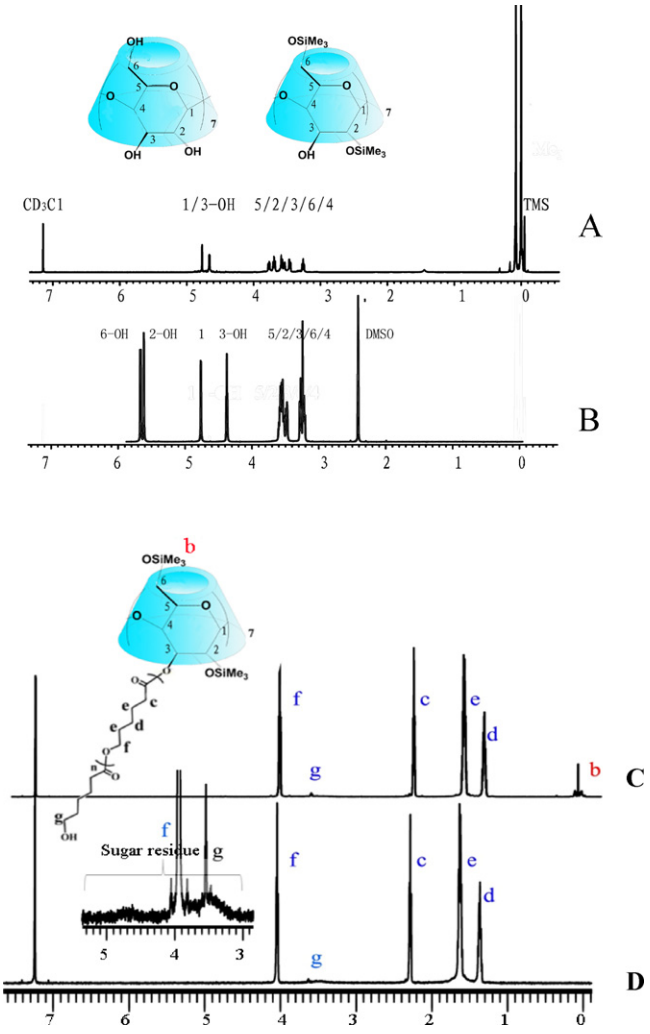

Fig. 1. ^{1}H NMR spectrum. (a) TMSCD (in $CDCl_3$); (b) β-CD (in DMSO-d6); (c) TMSCD-PCL_{18} (in $CDCl_3$); and (d) CD-PCL_{18} (in $CDCl_3$).

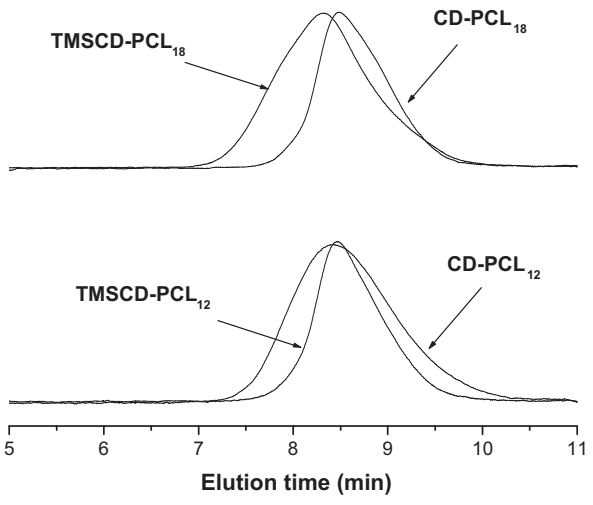

Fig. 2. GPC traces of TMSCD-PCL_{18}, CD-PCL_{18}, TMSCD-PCL_{12} and CD-PCL_{12}.

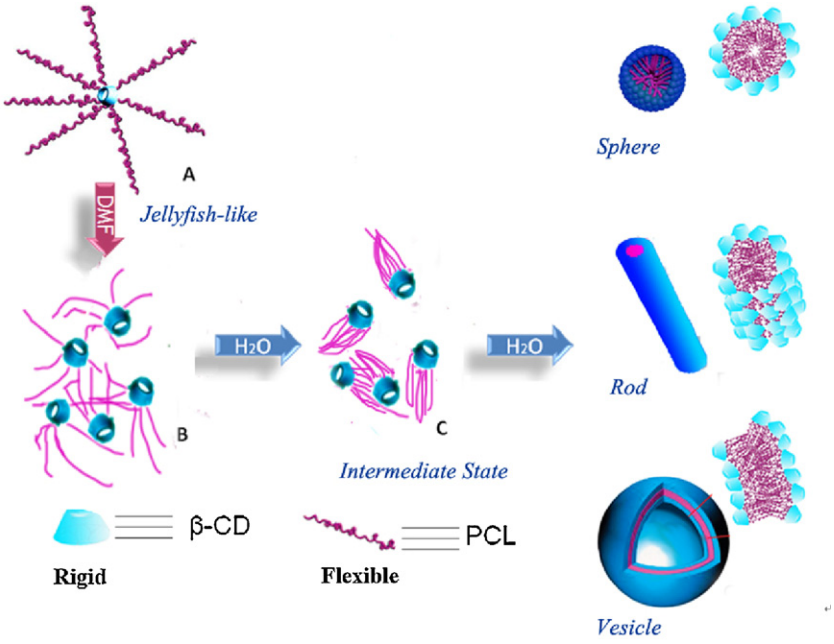

Scheme 2. A proposed mechanism leading to the self-assembled morphologies of amphiphilic rigid-coil copolymer CD-PCL in water.

Ydens (Ydens et al., 2000). One may assume that the voluminous PCL branches of the obtained TMSCD-PCL$_s$ spread all around the TMSCD backbone in $CDCl_3$ solution. So TMSCD glucose protons were partially screened in ^{1}H NMR spectra. Therefore, higher PCL content will lead to overestimated $\overline{DP_{PCL}}$ values measured by ^{1}H NMR spectroscopy, as observed in Table 1. The experimental conditions (120 °C and 24 h) allow high and sometimes even quantitative polymerization yields (Table 1), so it can thus be concluded that the initial feed molar ratio of CL and hydroxyl group of TMSCD$_{DS=71.9\%}$ is better suited than ^{1}H NMR to determine $\overline{DP_{PCL}}$, especially when the initial CL weight fraction is over 0.3.

In order to recover the protected hydroxyl groups on the β-CD backbone and avoid any damage to PCL moieties, the trimethylsilyl (TMS) ether groups had to be removed under mild condition. Herein, boron trifluoride diethyl etherate ($BF_3{\cdot}Et_2O$) was employed in the third step to cleave the trimethylsilyl groups of the TMSCD-PCL copolymers at room temperature. Thus, a series of CD-PCL$_s$ with different PCL branch lengths ($\overline{DP_{PCL}}$) were prepared and characterized by IR, ^{1}H NMR and GPC.

Fig. 1d exhibits a representative CD-PCL$_{18}$ ^{1}H NMR spectrum. It clearly shows that the proton signal of the —O—Si$(CH_3)_3$ groups at 0.1 ppm was not detected and the major proton signals of PCL chains and β-CD glucose residues remain essentially intact, suggesting that no degradation of the β-CD backbone and the PCL branches occurred.

The resulting TMSCD-PCL and CD-PCL in the above-mentioned three steps were characterized by GPC with tetrahydrofuran (THF) as the mobile phase and linear polystyrene as calibration standard. In Fig. 2 and Table 1, the GPC curves of the resulting TMSCD-PCL$_s$ and CD-PCL$_s$ copolymers with different PCL branch lengths reveal unimodal elution peaks, which suggest that no linear PCL formed. It should be noticed that $M_{n,GPC}$ values of the TMSCD-PCL$_s$ and CD-PCL$_s$ are also less than that of $M_{n,cal}$. It is well known that the molecular size of a polymer with cyclic or branched conformation is less than that of linear polymers with the same molecular weight. In our experiment, the molecular weight of the branched TMSCD-PCL and CD-PCL copolymers were measured with linear polystyrene as calibration standard. So it can be assumed that the resulting M_n^{GPC} values are less than the $M_{n,cal}$ values when linear polystyrene was used as calibration standard.

Thus, a rigid-coil CD-PCL copolymer with controlled branched structure was synthesized, in which flexible and hydrophobic PCL branches were selectively connected onto the wide side of the rigid and hydrophilic torus-shaped β-CD. Due to the protection/deprotection of TMS groups to the hydroxyl groups of the β-CD, the outer surface of the β-CD remains hydrophilic and the whole CD-PCL copolymer is amphiphilic, with a jellyfish-like topological structure as shown in Scheme 2.

It is reported that the crystalline property of amphiphilic copolymer influences hierarchical structure of its formed nanoparticles (Lin & Gast, 1996; Portinha, Bouteiller, Pensec, Richez, & Chassenieux, 2004; Richter et al., 1997; Wang, Li, Tao, Guo, & Yan, 2006). So the crystalline behavior of the obtained branched copolymers was investigated by DSC. Fig. 3 shows the second melting curves of the branched copolymers. PCL homopolymer is a crystalline polymer (M_n = 5000, the melting temperature T_m = 58.8 °C). Since β-CD did not show any melting transition, the detected thermal phenomenon in DSC can only be attributed to the PCL segment

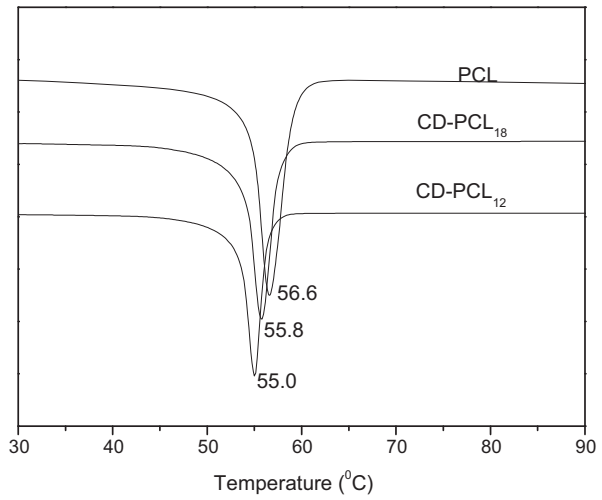

Fig. 3. DCS curves of the copolymers and PCL homopolymer with a rate of 10 °C/min at second heating run. (a) PCL homopolymer, (b) CD-PCL$_{18}$ and (c) CD-PCL$_{12}$.

in CD-PCL_s. It was observed that the two branched copolymers can also form crystal and the T_m values are lower than that of PCL homopolymer.

3.2. Self-assembled nanostructures of CD-PCL copolymer

The self-assembled aggregation in water of the amphiphilic rigid-coil CD-PCL copolymer with a unique jellyfish-like branched architecture was studied by an indirect method, where CD-PCL_{18} with long PCL branches was considered. CD-PCL_{18} copolymer was firstly dissolved in common solvent DMF to form a series of copolymer solution with different initial concentrations. Deionized water was then added dropwise to the CD-PCL_{18} solution under vigorous stirring until a desired amount of water was reached. After that, a large amount of water was added to the solution in order to quench the resulting morphologies. The solution was then dialyzed against water to remove the organic solvent. The critical aggregate concentration (CMC) of CD-PCL_{18} in water was measured by the fluorescent probe method (Fig. 4a). The CMC was chosen as the concentration when pyrene exhibited an apparent increase in the I_3/I_1 ratio with increasing concentration of the copolymer, indicating that the aggregation of the copolymer occurred. The results show that the CMC was about 1.2×10^{-3} mg/ml.

The morphology of the CD-PCL_{18} aggregates was observed by TEM. When the initial concentrations of CD-PCL_{18} in DMF varied from 0.01 to 8.0 mg/ml and the final concentration of the obtained aggregates solution in water was about in the range of 0.002–1.3 mg/ml, multiple self-assembled nanostructures were obtained (Fig. 5). When the initial concentration was 0.01 mg/ml, spherical micelles concomitant with a few short-rods were observed, as shown in Fig. 5a. The size of the CD-PCL_{18} aggregates was determined by DLS measurements, which gave a result of about 125 nm in average diameter (Fig. 4b). The spherical micelle is comprised of a shell of the hydrophilic β-CD and a dense core of hydrophobic PCL branches. This observation also showed that the copolymer tended to transform into rod-like micelles from spherical micelles, even at a low initial concentration. With increasing initial concentration, the CD-PCL_{18} aggregated into worm-like short rods and then long rods with an average diameters of 100 nm (Fig. 5b–d). After continuing to increase the initial concentration of 1.0 mg/ml, the micelles were converted to vesicles. The size of the CD-PCL_{18} aggregates was further determined by DLS measurements, which gave an average diameter of about 369 nm (Fig. 4b). It was observed that different vesicles trended to aggregate into vesicular clusters, as shown in Fig. 5e–g. And the vesicular clusters continued to aggregate into vesicular network (Fig. 5h and i) with further increase of the copolymer initial concentration (6.0–8.0 mg/ml). At this time, copolymer micelles precipitate out easily from the water. Interestingly, hierarchical structure formed in the vesicular network. At high magnification, the stripe structure of the vesicles could be clearly seen (Fig. 5j).

To get complementary information about the CD-PCL_{18} aggregates water solution, viscosity measurements were carried out (25 ± 0.1 °C). As shown in Fig. 4c, the wave-like variation of η_{sp}/c was observed with the increase of CD-PCL_{18} copolymers concentration in water. This behavior is similar to that of conventional low molecular mass surfactants and amphphilic copolymer. It is well known that η_{sp}/c of a conventional polymer in dilute solution increase monotonously with the increase of the polymer concentration. CD-PCL_{18} presents a "normal" variation of polymer solution in the first increase of η_{sp}/c as a function of c, showed that it is monomolecular in the region of very low concentrations. However, the insoluble PCL chains of CD-PCL copolymer in water begin to associate and form spherical micelles and lead to this initial decrease of η_{sp}/c, as the copolymer concentration increases. During this process, the solvent is progressively driven out of the micelle core, which would explain the swelling of the micelle near CMC. The plot then showed a slight variation of increase–decrease–increase–decrease when the copolymer concentration increases continuously, suggesting that

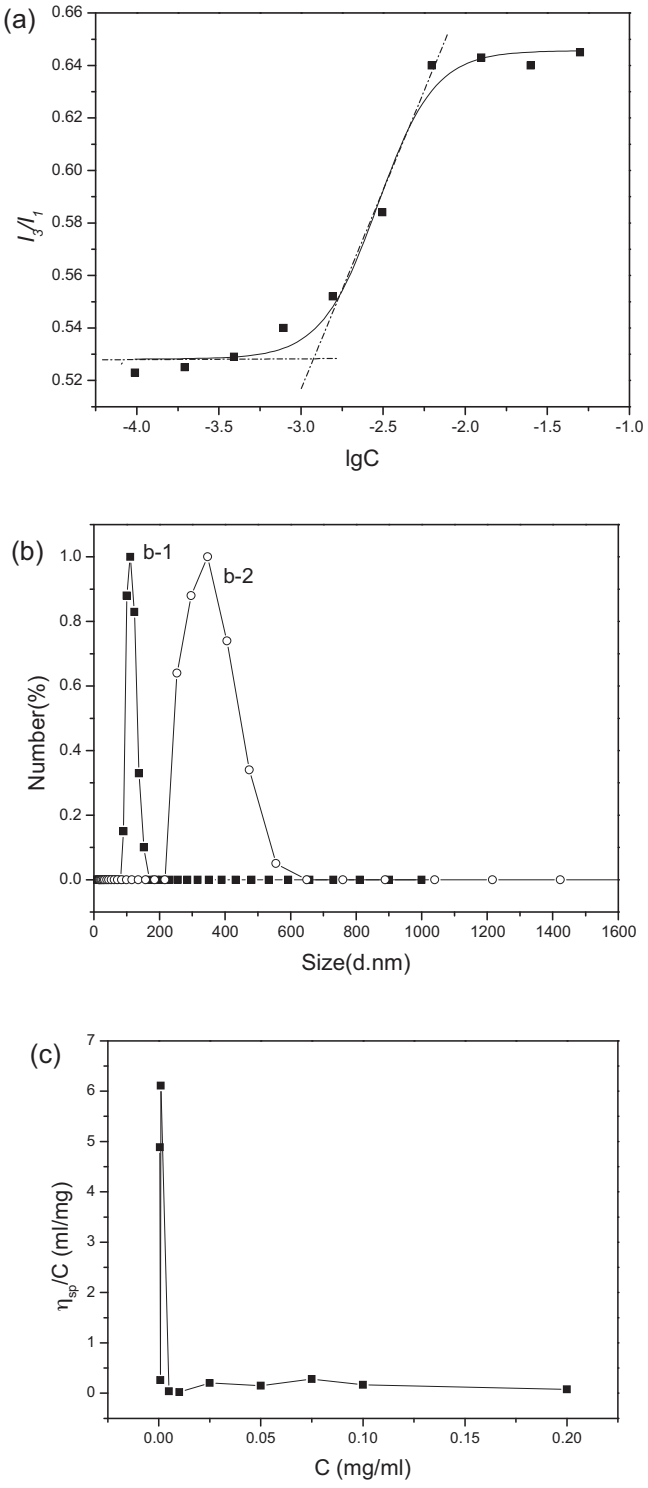

Fig. 4. The self-assembled properties of CD-PCL_{18} in water. (a) Determination of CMC using the fluorescent method with pyrene as a probe; (b) the DLS size distribution in water of the micelles with different initial DMF concentrations, (b-1) 0.01 mg/ml, (b-2) 1.0 mg/ml; (c) the η_{sp}/c of CD-PCL_{18} copolymers in water with different concentrations (25 ± 0.1 °C).

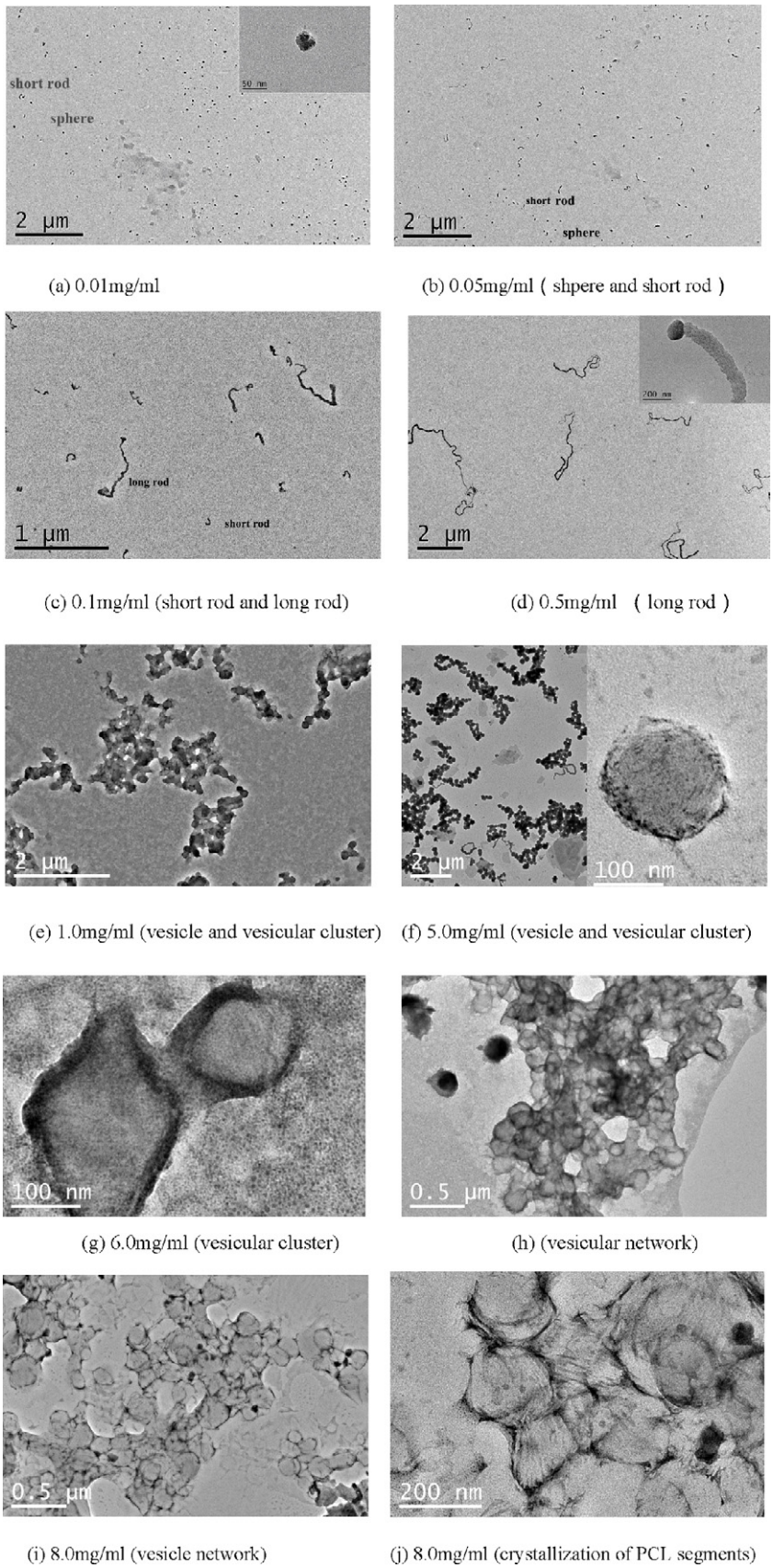

Fig. 5. TEM images of CD-PCL_{18} self-assembled micelles in water with different initial concentrations in DMF. (a) 0.01 mg/ml; (b) 0.05 mg/ml; (c) 0.1 mg/ml; (d) 0.5 mg/ml; (e) 1.0 mg/ml; (f) 5.0 mg/ml; (g) 6.0 mg/ml; (h) 6.0 mg/ml; (i)8.0 mg/ml; (j) 8.0 mg/ml.

the morphology of CD-PCL_{18} transfer from sphere to rod and then vesicle. The above results of viscometry gave additional validation on the micellar formation and the transformation of micellar morphology, which was corresponded with the obersvation of TEM.

Scheme 2 displays a possible self-assembled mechanism of the copolymers in aqueous solution. The synthesized amphiphilic CD-PCL_{18} has a unique rigid-coil branched structure, in which the flexible hydrophobic PCL branches were tied onto the wide side of rigid hydrophilic β-CD. Before the addition of water, the CD-PCL_{18} is unwound unimolecules in DMF and showed a jellyfish like morphology (Scheme 2A and B). Upon addition of the poor solvent water to the DMF solution of the copolymer, the solvent progressively becomes incompatible with the PCL branches. It is easy to understand that the PCL branches tied to a ring of β-CD firstly trend to aggregate together to form an intermediate state C in the dilute solution. At this time, the amphiphile behaves like a highly asymmetric diblock copolymer as shown in Scheme 2 C, in which the PCL chains tied to the ring of β-CD as a whole is treated as hydrophobic block and β-CD as hydrophilic block. Apparently, the formation of the intermediate state C increases the Flory-Huggins χ parameter of β-CD backbone and PCL branches and further drives the microphase separation of β-CD and PCL chains. At the same time, the self-assembly of the rigid-coil branched copolymers is directed not only by the microphase separation of the β-CD backbone and PCL branches but also by the tendency of the rigid β-CD to form crystalline domains. This competition process leads to the formation of self-assembled "crew-cut" micelles in which long PCL chains as hydrophobic core and short β-CD as hydrophilic shell. And with the increase of the initial concentration of CD-PCL_{18} copolymer in DMF, not only spherical micelles but also rod and vesicle nanostructures formed. Simultaneously, due to the protection/deprotection of TMS groups to the hydroxyl groups of the β-CD, there remain plenty of hydroxyl groups on the β-CD backbone on the vesicular shell so that hydrogen bonds among the vesicles may form when the initial concentration of the copolymer are increased to a certain extent. Consequently, the vesicles connected with each other to form cluster or network structure.

Interestingly, hierarchical structure formed in the vesicular network. It can be clearly seen that the strip of PCL segments (Fig. 5j). Similar hierarchical structure was also observed during the studies on self-assembly behavior of amphiphilic copolymer in a selective solvent. It is found that, if flexible blocks can crystallize, organized structure could form within the core of the formed micelles (Lin & Gast, 1996; Portinha et al., 2004; Richter et al., 1997; Wang et al., 2006). For example, poly(ethylene oxide)–polystyrene diblock copolymers in hydrocarbon solvents form thin platelet structures consisting of chain-folded crystalline domains of the insoluble block polystyrene. PCL homopolymer and CD-PCL copolymers are crystalline polymers whose melting temperatures are about 60 °C (Fig. 3). The fact suggests that the strong tendency of PCL to crystallize may be the main reason for the formation of the observed hierarchical stripe structure.

3.3. Inclusion of CD-PCL micelles to FcA

The inclusion of CD-PCL micelles to FcA was monitored by UV–vis spectroscopy. As shown in Fig. 6, the characteristic bands of FcA appear at 270 and 320 nm (Fig. 6a) and CD-PCL_{18} shows no peak at 270 and 320 nm. Compared with the spectrum of FcA and CD-PCL_{18}, the peak at 320 (Fig. 6b) of CD-PCL_{18}/FcA almost disappears and the peak at 270 nm becomes weak, suggesting that FcA was successfully encapsulated into the micelles.

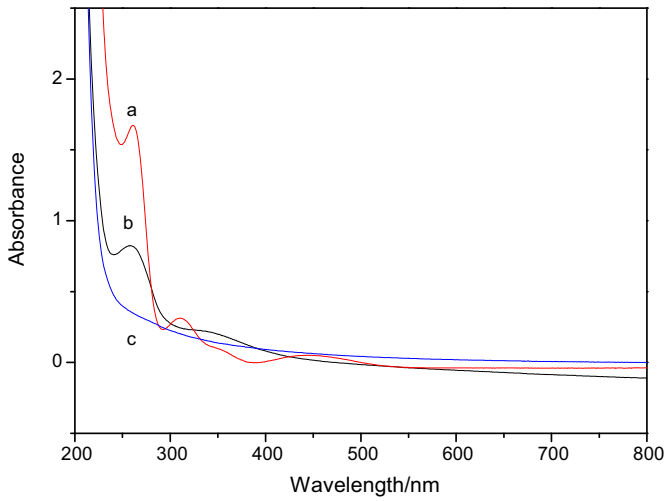

Fig. 6. UV–vis absorption spectra of FcA (a); CD-PCL_{18}/FcA (b); CD-PCL_{18} (c).

4. Conclusions

In this paper, a facile strategy to prepare biodegradable branched copolymers (CD-PCLs) was successfully developed through the combination of controlled ring-opening polymerization (CROP) and protection/deprotection technique of β-CD *via* trimethylsilyl groups. Here, biodegradable PCL as hydrophobic flexible branches was selectively connected onto the wide side of the hydrophilic rigid torus-shaped β-CD. The topological structure of the resulting rigid-coil CD-PCL copolymers looks like a jellyfish. The rigid-coil branched copolymers with unique "jellyfish-like" branched structures could self-assemble into multi-morphological aggregates in water such as spheres, rods, vesicles, vesicular clusters and vesicular network. Interestingly, hierarchical stripe structure was observed in the formed vesicular network, as being driven by the crystallization of PCL segment in micelles. Thus, a new route to form multi-morphological self-assembled structures was developed using amphiphilic cyclodextrin-based branched copolymer in water with biodegradable properties. These branched copolymers bearing reactive hydroxyl groups and ability to include guest molecules into the hydrophobic cavity of β-CD, which as well as the formed supramolecular aggregates should be useful as functional biomaterials for many potential applications such as drug delivery.

Acknowledgments

This research was financially supported by the Natural Science Foundation of China (Grant No. 20604033) and the Foundation of Graduate University of Chinese Academy of Sciences.

References

Agut, W., Brûlet, A., Schatz, C., Taton, D., & Lecommandoux, S. (2010). PH and temperature responsive polymeric micelles and polymersomes by self-assembly of poly[2-(dimethylamino)ethyl methacrylate]-b-poly(glutamic acid) double hydrophilic block copolymers. *Langmuir*, *26*, 10546–10554.

Akiyoshi, K., Deguchi, S., Tajima, H., Nishikawa, T., & Sunamoto, J. (1997). Microscopic structure and thermoresponsiveness of a hydrogel nanoparticle by self-assembly of a hydrophobized polysaccharide. *Macromolecules*, *30*, 857–861.

Breitenkamp, K., & Emrick, T. (2003). Novel polymer capsules from amphiphilic graft copolymers and cross-metathesis. *Journal of the American Chemical Society*, *125*, 12070–12071.

Borisov, O. V., & Zhulina, E. B. (2005). Amphiphilic graft copolymer in a selective solvent: Intramolecular structures and conformational transitions. *Macromolecules*, *38*, 2506–2514.

Cai, C., Lin, J., Chen, T., & Tian, X. (2009). Aggregation behavior of graft copolymer with rigid backbone. *Langmuir*, *26*, 2791–2797.

Chen, J. T., Thomas, E. L., Ober, C. K., & Mao, G.-p. (1996). Self-assembled smectic phases in rod-coil block copolymers. *Science*, *273*, 343–346.
Cheng, C.-X., Huang, Y., Tang, R.-P., Chen, E.-Q., & Xi, F. (2005). Molecular architecture effect on self-assembled nanostructures of a linear-dendritic rod triblock copolymer in solution. *Macromolecules*, *38*, 3044–3047.
Discher, D. E., & Eisenberg, A. (2002). Polymer vesicles. *Science*, *297*, 967–973.
Duan, H., Kuang, M., Wang, J., Chen, D., & Jiang, M. (2003). Self-assembly of rigid and coil polymers into hollow spheres in their common solvent. *Journal of Physical Chemistry B*, *108*, 550–555.
Gou, P.-F., Zhu, W.-P., & Shen, Z.-Q. (2010). Synthesis, self-assembly, and drug-loading capacity of well-defined cyclodextrin-centered drug-conjugated amphiphilic A14B7 miktoarm star copolymers based on poly(ε-caprolactone) and poly(ethylene glycol). *Biomacromolecules*, *11*, 934–943.
He, F., Gädt, T., Jones, M., Scholes, G. D., Manners, I., & Winnik, M. A. (2009). Synthesis and self-assembly of fluorescent micelles from poly(ferrocenyldimethylsilane-b-2-vinylpyridine-b-2,5-di(2-ethylhexyloxy)-1,4-phenylvinylene) triblock copolymer. *Macromolecules*, *42*, 7953–7960.
Hickey, R. J., Haynes, A. S., Kikkawa, J. M., & Park, S.-J. (2011). Controlling the self-assembly structure of magnetic nanoparticles and amphiphilic block-copolymers: From micelles to vesicles. *Journal of the American Chemical Society*, *133*, 1517–1525.
Ho, C.-C., Lee, Y.-H., Dai, C.-A., Segalman, R. A., & Su, W.-F. (2009). Synthesis and self-assembly of poly(diethylhexyloxy-p-phenylenevinylene)-b-poly(methyl methacrylate) rod-coil block copolymers. *Macromolecules*, *42*, 4208–4219.
Hu, Y., Jiang, X., Ding, Y., Ge, H., Yuan, Y., & Yang, C. (2002). Synthesis and characterization of chitosan-poly(acrylic acid) nanoparticles. *Biomaterials*, *23*, 3193–3201.
Jain, S., & Bates, F. S. (2003). On the origins of morphological complexity in block copolymer surfactants. *Science*, *300*, 460–464.
Jenekhe, S. A., & Chen, X. L. (1998). Self-assembled aggregates of rod-coil block copolymers and their solubilization and encapsulation of fullerenes. *Science*, *279*, 1903–1907.
Jenekhe, S. A., & Chen, X. L. (1999). Self-assembly of ordered microporous materials from rod-coil block copolymers. *Science*, *283*, 372–375.
Jeong, J. H., Kang, H. S., Yang, S. R., & Kim, J.-D. (2003). Polymer micelle-like aggregates of novel amphiphilic biodegradable poly(asparagine) grafted with poly(caprolactone). *Polymer*, *44*, 583–591.
Junnila, S., Houbenov, N., Hanski, S., Iatrou, H., Hirao, A., Hadjichristidis, N., et al. (2010). Hierarchical smectic self-assembly of an ABC miktoarm star terpolymer with a helical polypeptide arm. *Macromolecules*, *43*, 9071–9076.
Kikuchi, A., & Nose, T. (1996). Unimolecular-micelle formation of poly(methyl methacrylate)-graft-polystyrene in iso-amyl acetate. *Polymer*, *37*, 5889–5896.
Kim, K. H., Huh, J., & Jo, W. H. (2003). Wirelike micelle formed by a T-shaped graft copolymer with a rigid backbone. *Macromolecules*, *37*, 676–679.
Klok, H. A., & Lecommandoux, S. (2001). Supramolecular materials via block copolymer self-assembly. *Advanced Materials*, *13*, 1217–1229.
Kuroda, K., Fujimoto, K., Sunamoto, J., & Akiyoshi, K. (2002). Hierarchical self-assembly of hydrophobically modified pullulan in water. Gelation by networks of nanoparticles. *Langmuir*, *18*, 3780–3786.
Lee, M., Cho, B.-K., & Zin, W.-C. (2001). Supramolecular structures from rod-coil block copolymers. *Chemical Reviews*, *101*, 3869–3892.
Lin, E. K., & Gast, A. P. (1996). Semicrystalline diblock copolymer platelets in dilute solution. *Macromolecules*, *29*, 4432–4441.
Liu, C.-L., Lin, C.-H., Kuo, C.-C., Lin, S.-T., & Chen, W.-C. (2011). Conjugated rod-coil block copolymers: Synthesis, morphology, photophysical properties, and stimuli-responsive applications. *Progress in Polymer Science*, *36*, 603–637.
Neiser, M. W., Muth, S., Kolb, U., Harris, J. R., Okuda, J., & Schmidt, M. (2004). Micelle formation from amphiphilic cylindrical brush – Coil block copolymers prepared by metallocene catalysis. *Angewandte Chemie International Edition*, *43*, 3192–3195.
Nouvel, C., Frochot, C., Sadtler, V., Dubois, P., Dellacherie, E., & Six, J.-L. (2004). Polylactide-grafted dextrans: Synthesis and properties at interfaces and in solution. *Macromolecules*, *37*, 4981–4988.
Ouchi, T., Kontani, T., & Ohya, Y. (2003). Mechanical property and biodegradability of solution-cast films prepared from amphiphilic polylactide-grafted dextran. *Journal of Polymer Science Part A: Polymer Chemistry*, *41*, 2462–2468.
Park, J., Moon, M., Seo, M., Choi, H., & Kim, S. Y. (2010). Well-defined star-shaped rod-coil diblock copolymers as a new class of unimolecular micelles: Encapsulation of guests and thermoresponsive phase transition. *Macromolecules*, *43*, 8304–8313.
Philippova, O. E., Volkov, E. V., Sitnikova, N. L., Khokhlov, A. R., Desbrieres, J., & Rinaudo, M. (2001). Two types of hydrophobic aggregates in aqueous solutions of chitosan and its hydrophobic derivative. *Biomacromolecules*, *2*, 483–490.
Portinha, D., Bouteiller, L., Pensec, S., Richez, A., & Chassenieux, C. (2004). Influence of preparation conditions on the self-assembly by stereocomplexation of polylactide containing diblock copolymers. *Macromolecules*, *37*, 3401–3406.
Qiu, X-Y., Wang, C.-Q., Shen, J., & Jiang, M.-W. (2011). Controlled synthesis of amphiphilic rod-coil biodegradable maltoheptaose-graft-poly(ε-caprolactone) copolymers. *Carbohydrate Polymers*, *83*, 1723–1729.
Ren, T.-B., Feng, Y., Zhang, Z.-H., Li, L., & Li, Y.-Y. (2011). Shell-sheddable micelles based on star-shaped poly(E-caprolactone)-SS-poly(ethyl glycol) copolymer for intracellular drug release. *Soft Matter*, *7*, 2329–2331.
Richter, D., Schneiders, D., Monkenbusch, M., Willner, L., Fetters, L. J., Huang, J. S., et al. (1997). Polymer aggregates with crystalline core: The system polyethylene–poly(ethylenepropylene). *Macromolecules*, *30*, 1053–1068.
Rösler, A., Vandermeulen, G. W. M., & Klok, H.-A. (2001). Advanced drug delivery devices via self-assembly of amphiphilic block copolymers. *Advanced Drug Delivery Reviews*, *53*, 95–108.
Sato, Y.-i., Kobayashi, Y., Kamiya, T., Watanabe, H., Akaike, T., Yoshikawa, K., et al. (2005). The effect of backbone structure on polycation comb-type copolymer/DNA interactions and the molecular assembly of DNA. *Biomaterials*, *26*, 703–711.
Song, H., He, R., Wang, K., Ruan, J., Bao, C., Li, N., et al. (2010). Anti-HIF-1 antibody-conjugated pluronic triblock copolymers encapsulated with Paclitaxel for tumor targeting therapy Source. *Biomaterials*, *31*, 2302–2312.
Wang, C.-Q., Dong, Y.-P., & Tan, H.-M. (2003). Biodegradable brushlike graft polymers. I. Polymerization of caprolactone onto water-soluble hydroxypropyl cellulose as the backbone by the protection of the trimethylsilyl group. *Journal of Polymer Science: Part A: Polymer Chemistry*, *41*, 273–280.
Wang, C.-Q., Li, G.-T., & Guo, R.-R. (2005). Multiple morphologies from amphiphilic graft copolymers based on chitooligosaccharides as backbones and polycaprolactones as branches. *Chemical Communication*, 3591–3593.
Wang, C., Li, G., Tao, S., Guo, R., & Yan, Z. (2006). Crystalline and micellar properties of amphiphilic biodegradable chitooligosaccharide-graft-poly(ε-caprolactone) copolymers. *Carbohydrate Polymers*, *64*, 466–472.
Ydens, I., Rutot, D., Degée, P., Six, J.-L., Dellacherie, E., & Dubois, P. (2000). Controlled synthesis of poly(ε-caprolactone)-grafted dextran copolymers as potential environmentally friendly surfactants. *Macromolecules*, *33*, 6713–6721.
Yusa, S.-I., Sakakibara, A., Yamamoto, T., & Morishima, Y. (2002). Reversible pH-induced formation and disruption of unimolecular micelles of an amphiphilic polyelectrolyte. *Macromolecules*, *35*, 5243–5249.
Zhang, L., & Eisenberg, A. (1996). Multiple morphologies and characteristics of crew-cut micelle-like aggregates of polystyrene-*b*-poly(acrylic acid) diblock copolymers in aqueous solutions. *Journal of the American Chemical Society*, *118*, 3168–3181.